

Kinematic Modelling: How sensitive are aerosol-cloud interactions to microphysical representation

Adrian Hill

Co-authors: Ben Shipway, Ian Boutle, Ryo Onishi

UK Met Office

Abstract

This work discusses how a simple kinematic model can be used to i) understand the behaviour of various warm-rain parametrisations and ii) understand aerosol-cloud-precipitation interactions within those warm-rain parametrisations. It will be demonstrated that the response of simulated precipitation to changes in aerosol is closely tied to the warm-rain parametrisation. It will also be shown how the results from simple kinematic simulations relate to large-scale models.

1. Introduction

Recent cloud resolving model (CRM) intercomparisons, particularly those focused on boundary layer clouds have highlighted a large spread in important simulated parameters such as surface precipitation rate and liquid water content (e.g. Ackerman et al, 2009; vanZantern et al, 2012). vanZantern et al (2012) showed that during the recent Rain In Cumulus over the Ocean (RICO) CRM intercomparison there were orders of magnitude difference in surface precipitation rates for drizzling shallow cumulus. Such a range could not be directly attributed to different choices in the complexity of the microphysics (e.g. 1M, 2M or bin) nor could it be attributed to the dynamics (e.g. grid resolution, numerical diffusion) or a combination of the two. In this work, we demonstrate how kinematic modelling, in particular the Kinematic Driver (KiD) model, can be used to isolate differences between microphysics parameterisations by constraining dynamics. The KiD model is employed to i) demonstrate the behaviour of various warm-rain parametrisations for one cloud drop number concentration and ii) investigate the sensitivity of precipitation to changes in cloud drop interactions with various warm-rain parameterisations in the absence of dynamic feedbacks.

2. Kinematic Driver (KiD) Model (Shipway & Hill, 2012)

The Kinematic Driver (KiD) model has been specifically developed as a simple microphysics interface to a common dynamic core, in which consistent testing of microphysics schemes can be performed. The KiD model is a community tool, which is free to download (see <http://appconv.metoffice.com/microphysics/index.shtml> for the code, documentation and list of publications). Shipway and Hill (2012) used the KiD model to perform an intercomparison of single moment (1M) and double moment (2M) bulk warm rain microphysics schemes (Table 1). Simulations from these bulk schemes were compared to a results from the Tel-Aviv University (TAU) size-bin resolved microphysics scheme (Tzivion et al. 1987). The TAU scheme is assumed to be the best microphysical estimate and as such, in this work, provides a baseline to which all other schemes are compared.

Table 1. Description of the bulk microphysics schemes tested. μ is the shape parameter for the scheme and N_0 is the intercept parameter, used to define the cloud drop size distribution. Swann (1998) is the modified Kessler scheme, KK2000 is from Khairoutdinov and Kogan (2000).

Description	Mass diameter and size spectra relations	Autoconversion	Fall speed constants
Single moment (1M)			
LEM 1M (LEM 2.4sm)	$N_a = 1.1e^{15}$, $N_b = 0.0$ $\mu = 2.5$	Swann (1998)	$a_r = 362.0$, $b_r = 0.65$ $f_r = 0.0$, $g_r = 0.5$
UM operational 1M (UM 7_3)	$N_a = 26.6$, $N_b = 1.57$ $\mu = 0.0$	Trippoli and Cotton (1980)	$a_r = 386.8$, $b_r = 0.67$ $f_r = 0.0$, $g_r = 0.4$
Thompson 1M* (Thompson07)	$N_2 = 2e^6$, $N_1 = 9e^9$ $\mu = 0.0$	Berry and Reinhardt (1974) (modified)	$a_r = 4854$, $b_r = 1$ $f_r = 195.0$, $g_r = 0.5$
Double moment (2M)			
LEM 2M (LEM 2.4dm)	$\mu = 2.5$	Swann (1998)	$a_r = 362.0$, $b_r = 0.65$ $f_r = 0.0$, $g_r = 0.5$
Thompson 2M* (Thompson09)	$\mu = 0.0$	Berry and Reinhardt (1974) (modified)	$a_r = 4854$, $b_r = 1$ $f_r = 195.0$, $g_r = 0.5$
Morrison 2M* (Morrison)	$\mu = 0.0$	KK2000	$a_r = 841$, $b_r = 0.8$ $f_r = 0.0$, $g_r = 0.54$

*The Thompson 1M, Thompson 2M and Morrison 2M are as made available with Weather Research * Forecasting Model (WRF) version 3.1, with some minor bug correction added.

2.1. Intercomparison set-up

The microphysics schemes (Table 1) were compared using the KiD standard test case warm1, which provides a simple updraft that is constant in height, to advect vapour and hydrometeors. The strength of the updraft follows a half-period of a sinusoid peaking at w_1 , after which there is no further forcing of the microphysical and thermodynamic fields. The temperature field is kept fixed throughout the simulation so as to minimise feedback from the different microphysical schemes. The updraft velocity is given as

$$w(z,t) = \begin{cases} w_1 \sin(\pi / t_1), & \text{if } t < t_1 \\ 0.0 & , \text{if } t > t_1 \end{cases}$$

Where $t_1 = 600$ s. With this case we compare the schemes using two updrafts, i.e. $w_1 = 2 \text{ m s}^{-1}$ (W2) and $w_1 = 3 \text{ m s}^{-1}$ (W3). The initial vapour and potential temperature fields are idealised profiles based on RICO.

2.2. Results from intercomparison

Figure 1 shows that for both W2 and W3 the 1M schemes tend to rain too early relative to the TAU scheme but the precipitation peaks are approximately the same for all schemes, except thompson07. Figures 1b and d show that increasing the microphysical complexity from 1M to 2M rain, tends to improve the timing of the onset of precipitation. The 2M schemes tend to over-predict the peak precipitation rate, however, particularly in the deeper cloud associated with W3. Shipway and Hill (2012) argue that the poor simulation of peak precipitation in the 2M schemes is the result of

excessive size sorting. To correct this, a new multi-moment bulk microphysics scheme “4A” was developed, which includes a third moment of the particle size distribution (PSD). Figure 2 shows that using a 3M scheme, where the 3rd moment is radar reflectivity, captures the change in PSD as rain sediments which results in better agreement between the bulk scheme and the TAU scheme.

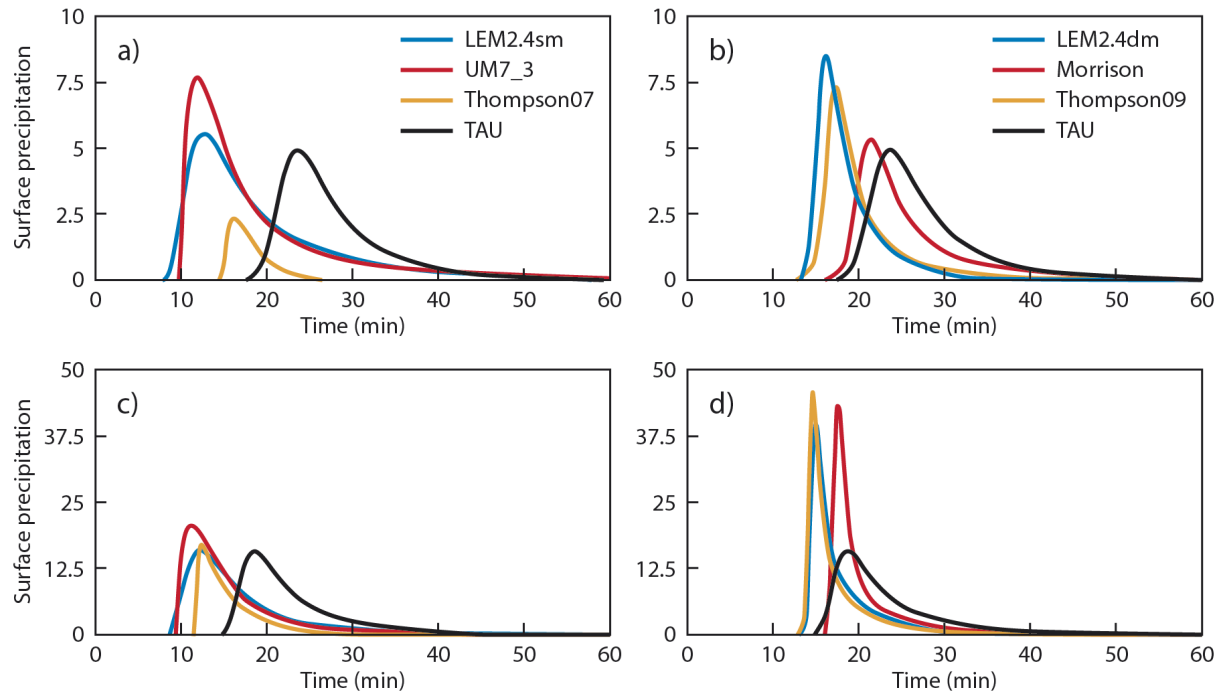


Figure 1: surface precipitation rate (mm hr-1) from W2 (a and b) and W3 (c and d). a and c show the comparison of the 1M schemes with the TAU scheme, while b and d show the comparison of the 2M schemes with TAU.

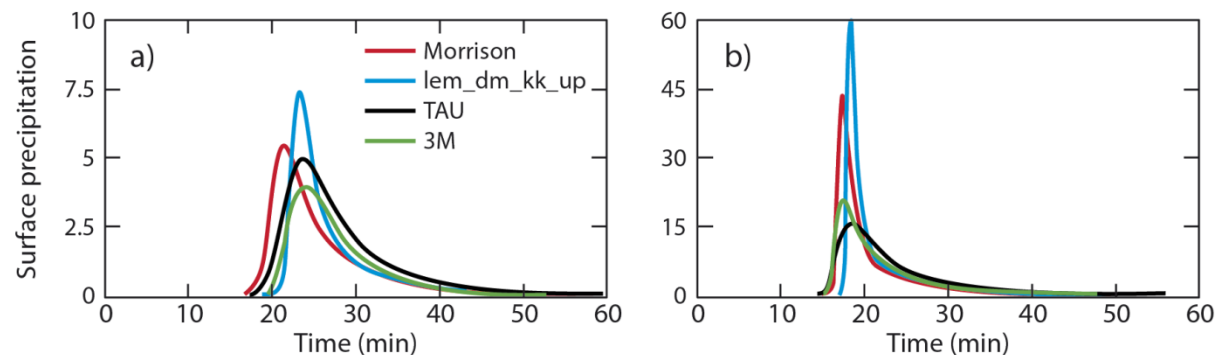


Figure 2: surface precipitation rate (mm hr-1) from W2 (a) and W3 (b).

While the surface precipitation produced by the 1M schemes show better agreement with the TAU scheme, Shipway and Hill (2012) show that the 1M schemes tend to generate too much of the rain by the autoconversion parametrisation. The 2M schemes produce more rain by accretion of cloud drops by rain and much less by autoconversion, which is in better agreement with the TAU scheme. Shipway and Hill (2012) therefore demonstrated how a simple kinematic model can be used to understand the individual process behaviour of different microphysics schemes, as well as be used as a vital tool for the development and testing of new schemes.

3. How do bin microphysics schemes compare?

In Shipway and Hill (2012) the TAU bin microphysics scheme was used as a “best estimate” to which all bulk schemes are compared. This is a sensible comparison because i) bin microphysics schemes are generally considered the best numerical representation of cloud microphysics and ii) the bulk schemes are either developed using output from bin microphysics (e.g. Khairoutdinov and Kogan, 2000) or bulk schemes are validated against output from bin schemes (e.g. Thompson et al, 2007). An important question to ask, however, is how do various bin microphysics compare? In an initial attempt to answer this we have compared the TAU simulation of W2 and W3 with MSSG simulations of W2 and W3. The MSSG scheme is described in Onishi and Takahashi (2012) and the simulations presented here were performed by Ryo Onishi.

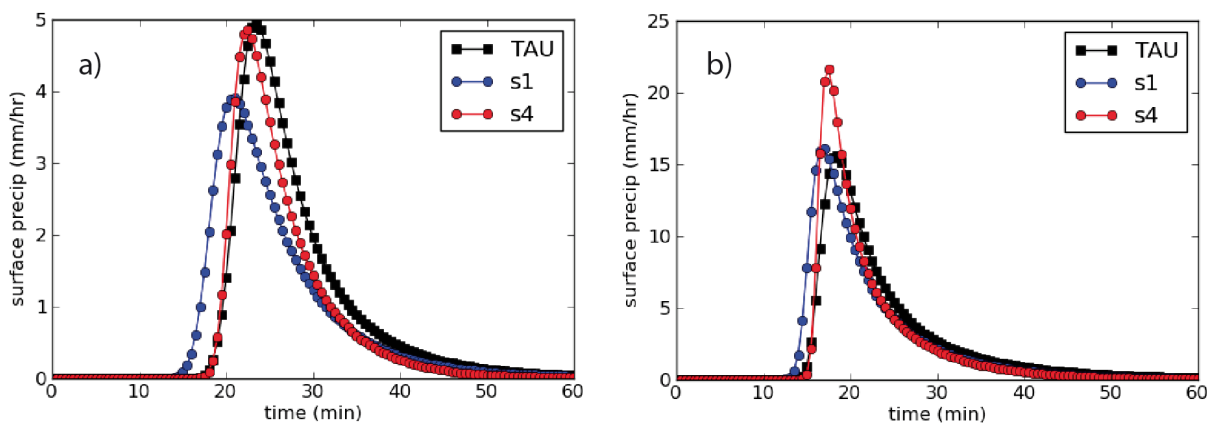


Figure 3. Comparison of the surface precipitation for a) W2 and b) W3 from the TAU double moment bin scheme with the MSSG single moment bin scheme (S1 and S4). S1 uses 34 bins, which is equivalent to the number of bins in TAU, while S4 uses 128 size bins.

Figure 3 shows that the surface precipitation produced by these two independently developed bin microphysics codes shows good agreement for both test cases. The agreement is particularly good when compared to the bulk comparison presented in Shipway and Hill (2012). The WMO/GASS microphysics intercomparison intends to address this by comparing more bin microphysics schemes, as well as aerosol processing in the cloud. For more information about this intercomparison see <http://slayoo.github.com/icmw2012-case1/>

4. Aerosol-cloud interactions in the KiD model

Section 2 and 3 show the behaviour of various schemes for one cloud drop number concentration (Nd). The response of precipitation to changes in aerosol loading and Nd remains a major uncertainty in climate and weather prediction (IPCC, 2007). In general this uncertainty results from

1. the complexity of the processes and the large range of spatial scales involved mean that parametrisations of aerosol and cloud microphysics are uncertain
2. dynamical and radiative feedbacks can result in “buffering” within a system (Stevens and Feingold, 2009), which can lead to unexpected responses

Here we present an investigation of point (1) by analysing multiple KiD simulations, to understand how precipitation produced by different cloud microphysics schemes respond to changes in aerosol or Nd when dynamics are constrained.

4.1. Test-case setup to model aerosol-cloud interactions in the KiD model

To investigate the response of simulated precipitation to changes in aerosol or cloud drop number concentration (Nd), we employ the test case used in Shipway and Hill (2012), e.g. W2 and W3, with the following changes

- w_1 ranges from 0.1 to 4.5 m s⁻¹, increasing by increments of 0.1 m s⁻¹, with one simulation for each updraft
- initial aerosol or N_d ranges from 20 to 300 cm⁻³, i.e., clean to polluted conditions, increasing by increments of 10 cm⁻³, with one simulation for each number concentration.

By varying w_1 and initial number concentration in this manner, we perform 1189 simulations with each scheme. This equates to 1189 clouds with varying LWP, i.e. increasing w_1 results in an increase in the maximum LWP, and varying number concentrations. The schemes used in this intercomparison are UM vn7.6 (the same as vn7.3), Thompson09, Morrison and TAU. In addition, we include simulations with the 4A scheme which use 2M cloud and 2M rain (4A_2M) and 2M cloud and 3M rain (4A_3M).

4.2. Aerosol-cloud interactions in the KiD model: Results

Figure 4 shows the maximum surface precipitation rate and the timing for the onset of that maximum plotted against liquid water path (LWP). Irrespective of the microphysics scheme, increasing LWP results with an increase in the maximum precipitation rate. Figure 4a shows that the sensitivity of the maximum precipitation rate to increasing N_d in the TAU scheme is largest at low LWP. For example, when LWP is less than 1 kg m⁻², a change in N_d from 20 to 300 cm⁻³ can result in up to a two orders of magnitude change in the maximum precipitation. As LWP increases the sensitivity to changes in N_d decreases. In a similar fashion, the timing of the peak precipitation is most sensitive to changes in N_d when LWP is low, with the timing and sensitivity to N_d decreasing with increasing LWP (Figure 4b).

In general, the 4A bulk scheme, with 2M cloud and 2M rain, and the Morrison bulk scheme, with 1M cloud and 2M rain produce similar qualitative behaviour to the TAU scheme when considering the sensitivity to changes in N_d and LWP. It is noted however, that the timing of the peak precipitation is earlier in the both bulk schemes, particularly when is N_d large. The peak precipitation rate and timing produced by 1M UM 7.6 scheme shows very little sensitivity to changes in N_d (Figures 4g and h). Furthermore, although the peak precipitation rate increases with increasing LWP, the timing of the peak shows relatively little change with increasing LWP.

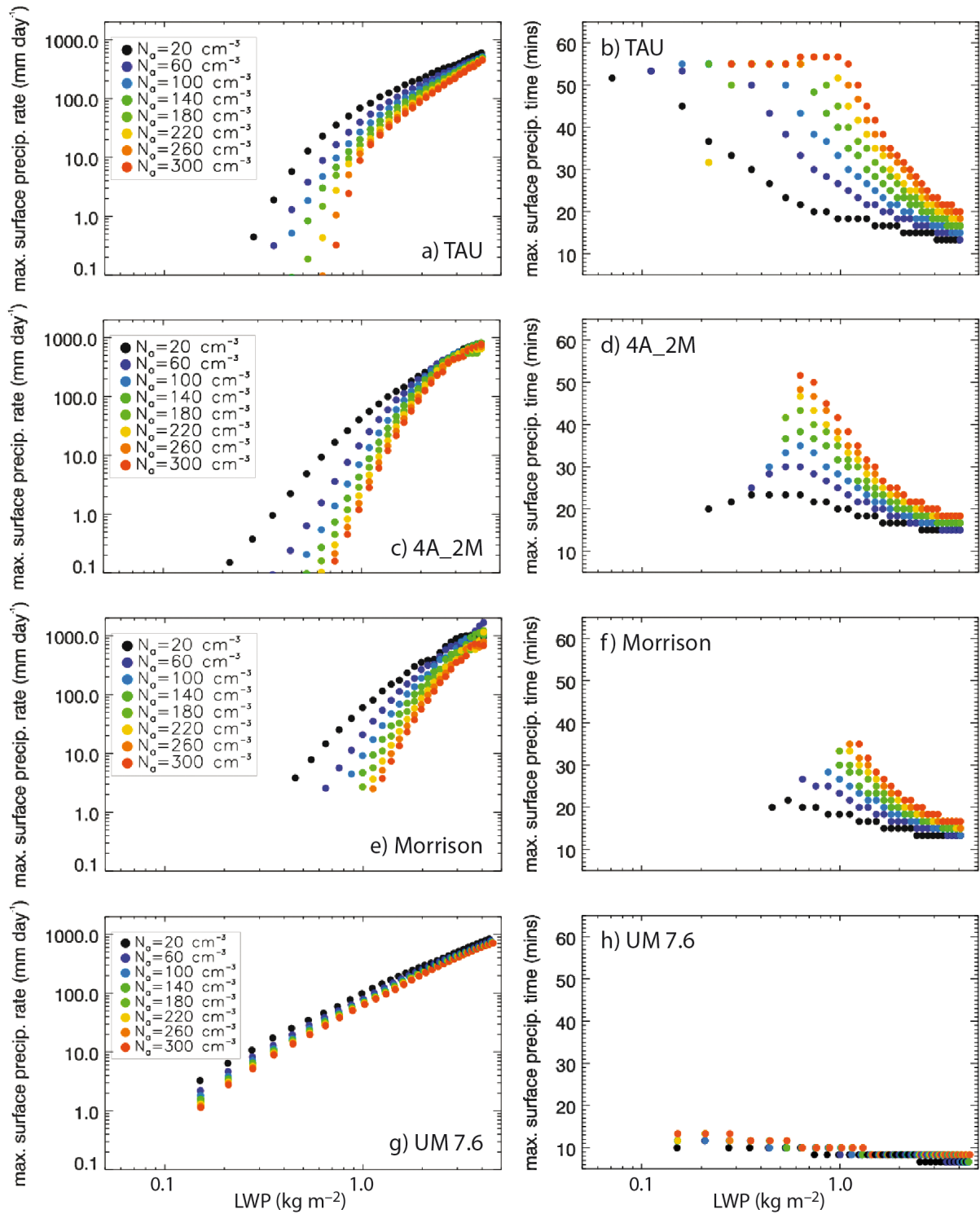


Figure 4. The maximum surface precipitation rate versus LWP (left hand column) and the time for the occurrence of maximum surface precipitation versus LWP (right hand column).

As the simulations presented here are kinematic, the large variation in sensitivity of precipitation to changes in N_d between the 2M and 1M schemes (Figure 4) is solely related to the microphysics scheme and parametrisation. Changing N_d in these bulk microphysics schemes only directly influences the precipitation formation and rate through the autoconversion parametrisation, i.e. the numerical method by which cloud water is initially converted to rain water. The 4A_2M and Morrison

scheme both use the Kogan and Khairoutdinov (2000) autoconversion (KK2000) scheme. The UM 7.6 1M scheme uses the Tripoli and Cotton (1980) autoconversion (TC) scheme. In order to understand the lack of sensitivity to changes in N_d in the UM 7.6 1M we run two more sets of simulations. The first set of simulations use the standard UM 7.6 scheme with TC autoconversion but the autoconversion efficiency (E_c) is reduced from 0.55 to 0.01. The second set uses the “warm rain” package in the UM 7.6 scheme. The “warm rain” package, which includes the Abel and Shipway (2007) fall-speeds, Abel and Boutle (2012) rain particle size distribution and the KK2000 autoconversion and accretion, was developed to deal with a tendency in the UM to rain too frequently in marine Sc (Boutle and Abel, 2012). Figure 5 shows the maximum precipitation rate and the timing of the rate versus LWP from these simulations. Dramatically reducing E_c results in a small increase in the sensitivity of the maximum precipitation rate (Figure 5a) and an increase in the sensitivity of the peak precipitation timing is clear (Figure 5b). It is noted that the number of simulations that produce surface precipitation is significantly reduced by reducing E_c relative to other schemes. Using the “warm rain package” results in an increase in the sensitivity of peak precipitation (Figure 5c) and timing (Figure 5d) so that the 1M scheme qualitative behaviour is closer to the more complex schemes. This shows how the KiD model can be used to develop, test and understand parametrisations efficiently.

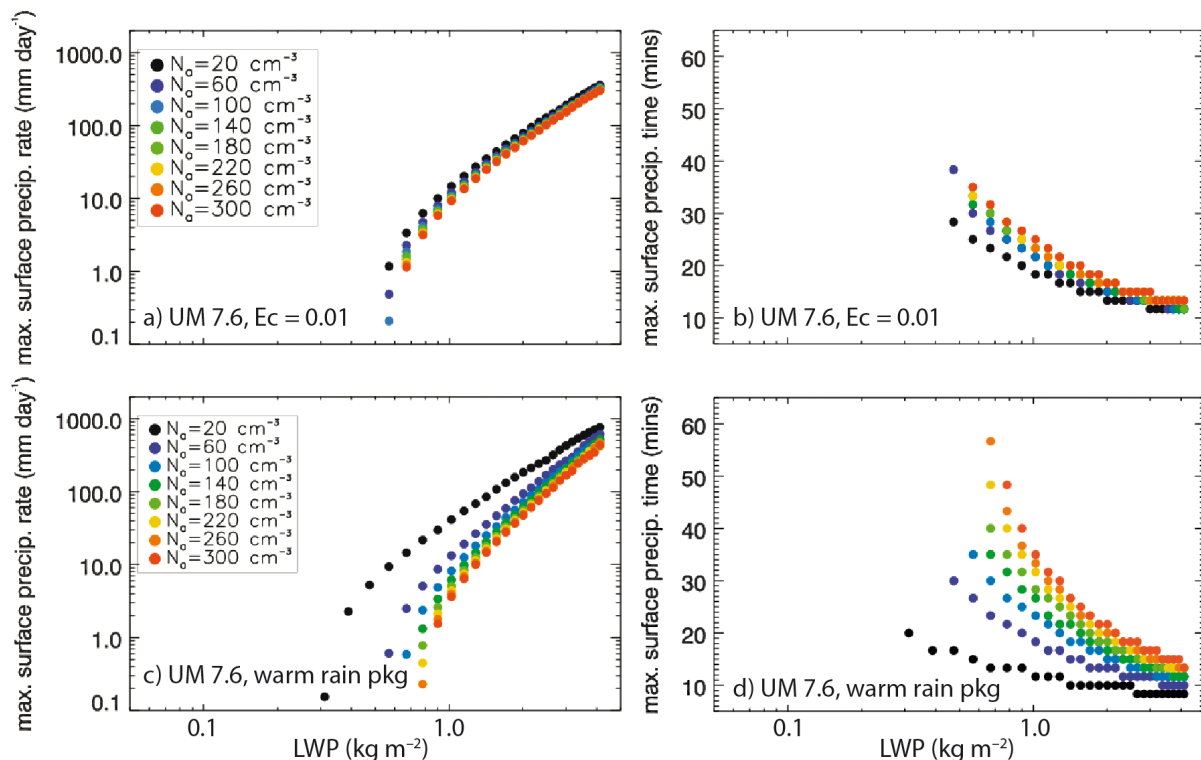


Figure 5. Same as Figure 4 for UM 7.6 $E_c=0.01$ (a and b) and UM 7.6 warm rain (c and d)

4.3. Precipitation Susceptibility

Figures 4 and 5 present all the precipitation data from the KiD simulations on two plots for each scheme. This presentation is a useful demonstration of a schemes overall behaviour when considering precipitation, but it is hard to compare schemes unless there are obvious large differences. In an effort to compare schemes we propose using the construct of precipitation susceptibility (S_0), which was introduced as a framework to investigate aerosol effects on precipitation by Feingold and Seibert (2009). S_0 is defined as follows

$$S_0 = -\frac{d \ln R}{d \ln N_d}$$

where R is precipitation rate and N_d is cloud drop number concentration.

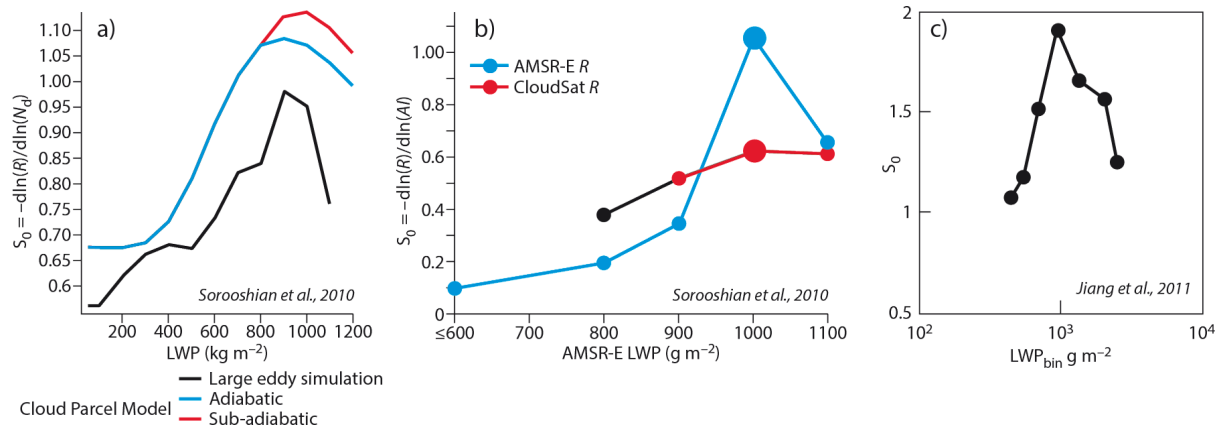


Figure 6. Precipitation susceptibility (S_0) versus LWP from Sorooshian et al 2010 and Jiang et al 2011

Figure 6 shows the behaviour of S_0 versus LWP for parcel simulations and LES and satellite observations (Feingold and Seibert, 2009; Jiang et al, 2011; Sorooshian et al, 2010). This shows that S_0 tends to initially increase with an increase in LWP and then S_0 decreases with increasing LWP. This demonstrates that precipitation from a lower LWP is more sensitive to changes in N_d , than that from a higher LWP. Such a trend is similar to the behaviour shown in Figure 4.

In this work S_0 is used to compare the relative response of different microphysics schemes to changes in N_d . S_0 is calculated as follows;

1. For each scheme, bin accumulated surface R and the maximum N_d for each KiD simulation into LWP bins (width of LWP bin = 100 g m^{-2})
2. Perform a linear regression in each bin to find a best fit for $\ln R$ against $\ln N_d$
3. Calculate S_0 in each bin using the fitted $\ln R$ and plot against LWP

Figure 7 shows the cloud base and surface S_0 for the single moment and multi-moment bulk schemes and the TAU bin scheme. At cloud base, the TAU bin scheme produces an S_0 that increases from 0.7 in the lowest LWP bin ($\text{LWP} = 100 \text{ g m}^{-2}$) to a maximum S_0 of 1.6 when $\text{LWP} = 600 \text{ g m}^{-2}$, then S_0 decreases less than 0.2 by 2000 g m^{-2} . Such a non-monotonic behaviour is qualitatively similar to that highlighted in Feingold and Seibert (2009), although the simulations presented here produce the

maximum S_0 at a lower LWP. In the TAU scheme, only LWP path bins larger than 400 g m^{-2} produce a rainfall rate at the surface that is above the threshold for analysis (0.05 mm day^{-1}), so S_0 is only calculated for LWP bins larger than this. The surface S_0 from the TAU scheme shows good agreement with the cloud base S_0 .

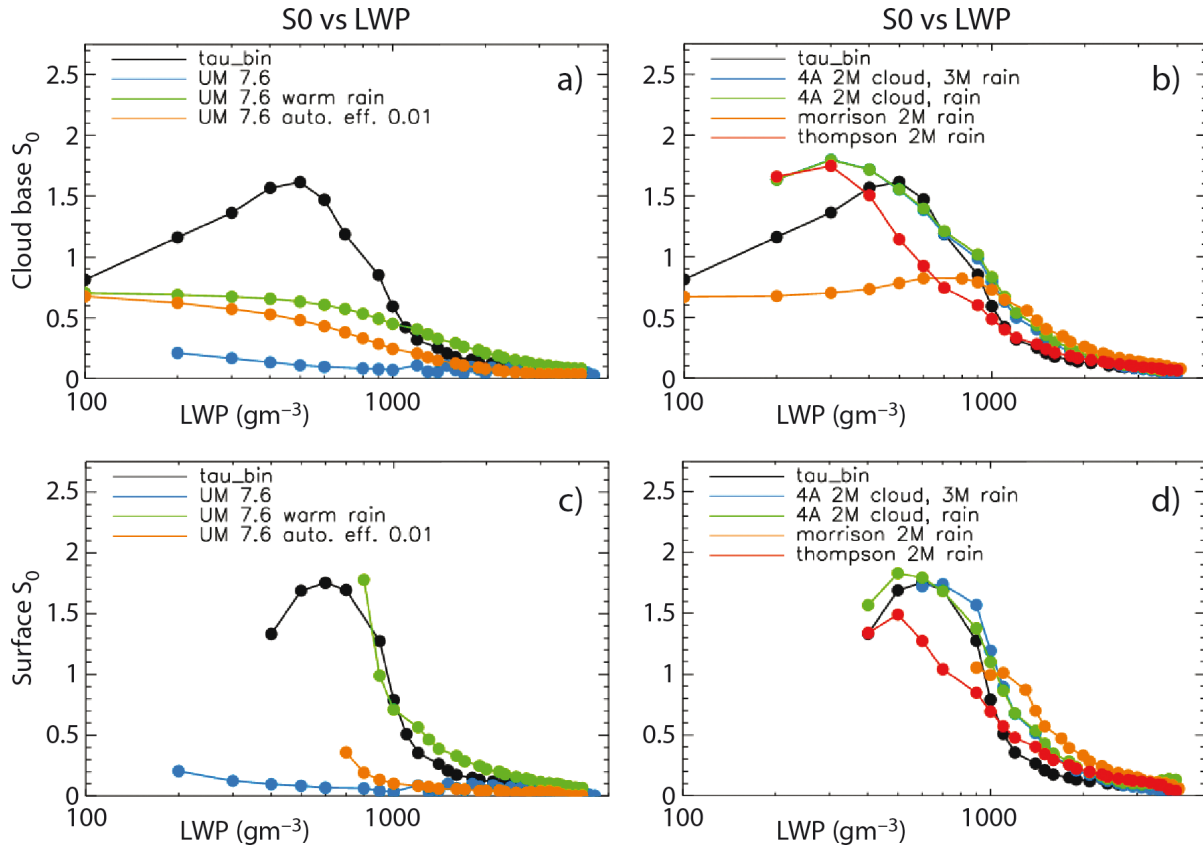


Figure 7. Cloud base S_0 versus LWP (top row) and surface S_0 versus LWP (bottom row). The left column shows the 1M scheme comparison with TAU scheme while the right column shows the comparison of the multi-moment bulk schemes to the TAU scheme

Figure 7a shows that all the versions of UM7.6 1M scheme produce lower susceptibility than the TAU scheme at cloud base. All versions of UM7.6 fail to produce an increase in S_0 with increasing LWP, when LWP is less than 600 g m^{-2} . As should be expected from Figure 4 and 5, the standard UM7.6 produces the lowest S_0 , and so it is relatively insensitive to changes in N_d for the simulations presented in this work. Using the warm rain package leads to an increase in S_0 . At the surface, the difference between the S_0 produced by the various UM versions is much larger than at cloud base, with UM 7.6 still producing relatively little sensitivity to changes in N_d , while UM 7.6 “warm rain” appears to show better agreement with the TAU scheme (Figure 7c), where S_0 is calculated.

The multi-moment bulk schemes tend to produce S_0 at cloud base that is in better agreement with the TAU scheme than the 1M scheme tested here (Figure 7b). There is, however, still a wide range in behaviour in S_0 versus LWP between the schemes. At the surface, the multi-moment schemes show good agreement with the TAU scheme as well as each other (Figure 7d). While Figure 7 shows the integrated precipitation rate for the KiD simulation, the trends for all schemes are comparable if the maximum or mean precipitation rate are analysed.

This section has described how precipitation susceptibility can be applied to multiple kinematic simulations to understand the response of different microphysics schemes to changes in N_d in the absence of dynamical feedbacks. Figure 7 suggests that increasing warm rain microphysical complexity can improve the relative response of precipitation to changes in N_d when compared to a bin microphysics scheme. It is interesting to note that while the TAU scheme produces similar S_0 versus LWP trends for the cloud base and surface, the bulk schemes produce very different trends at the cloud base and surface. This suggests that S_0 and its evolution with altitude is sensitive to cloud microphysics parameterisation, in particular it is sensitive to the representation of the rain, i.e. the PSD, sedimentation and associated evaporation. It is important to note that S_0 only captures the relative response of a precipitation rate to changes in N_d ; it includes no information about the timing of a precipitation event, which is an important parameter for both NWP and high-resolution regional and global climate prediction.

5. Do the KiD results mean anything?

Up to this point the KiD model has been used as a stand-alone model for developing, debugging and assessing various microphysics schemes. The results identify underlying microphysical behaviours and interactions within each scheme that may be relevant to CRM, high resolution NWP and GCM. To investigate this further, we have performed following two GCM simulations with the Met Office UM

1. UM GCM simulation with the GA (Global Atmosphere) 4.0 configuration in which the microphysics is equivalent to UM7.6 in KiD
2. UM GCM simulation with the GA 4.0 configuration and “warm rain” package, upscaled to GCM as described in Boutle et al (2013)

Figure 8 shows the global 10 year mean of large-scale precipitation (non-convective) with the GA 4.0 configuration and UM 7.6 microphysics (Figure 8a) and the “warm rain” package (Figure 8b). Figure 8a shows that there is a widespread coverage of low rain rates, which is a known issue with such a UM configuration (see Abel and Boutle, 2012b for further discussion). Figure 8b shows that using the “warm rain” package results in a reduction in the coverage of large-scale precipitation, particularly in the tropics and subtropics.

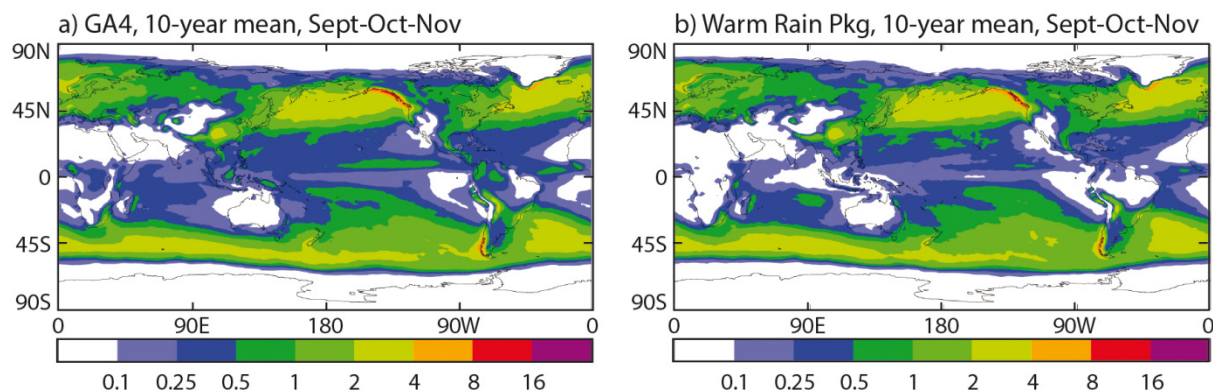


Figure 8. 10 year mean of large-scale (non-convective) precipitation

Figure 9 focuses on the South-East Pacific region of these simulations and shows that the “warm rain” package results in less rain in high aerosol regions, i.e. coastal regions, and an increase in rain in low aerosol regions, i.e. remote marine regions.

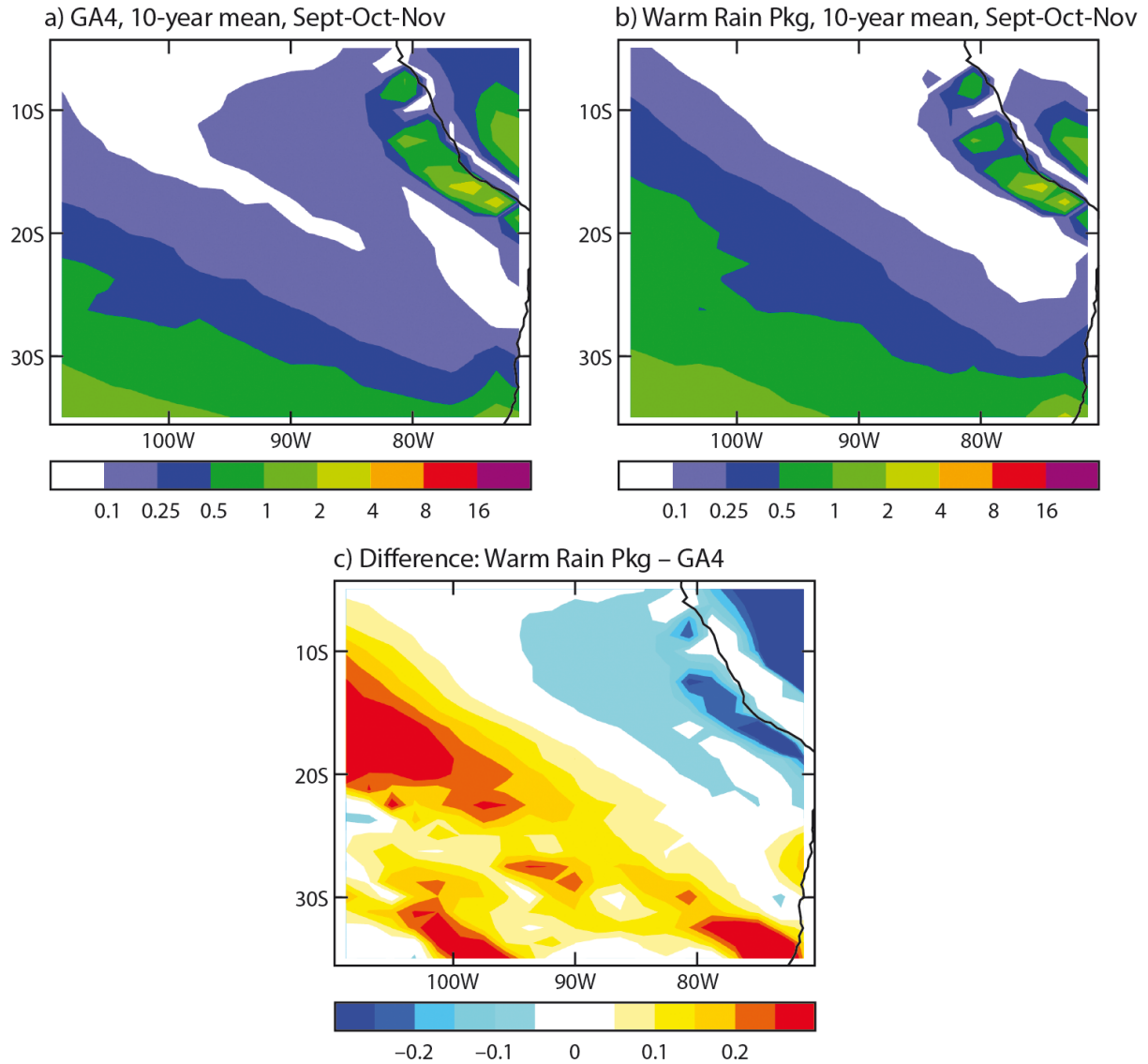


Figure 9. 10 year mean large-scale (non-convective) precipitation over the South-East Pacific region.

These results compare well with Abel and Boutle (2012) and correspond with the conclusions from the KiD simulations. Figure 10 shows the precipitation susceptibility calculated from the GCM simulations. It is clear that even though the GCM includes all parametrisations and feedbacks, the trend in S_0 of large-scale (non-convective) precipitation to changes in N_d are similar to those identified with the KiD simulations, i.e. the GA4.0 configuration with TC autoconversion produces very little sensitivity to changes in N_d while the “warm rain” package produces a trend that is qualitatively comparable to that simulated by more complex microphysics schemes and observations.

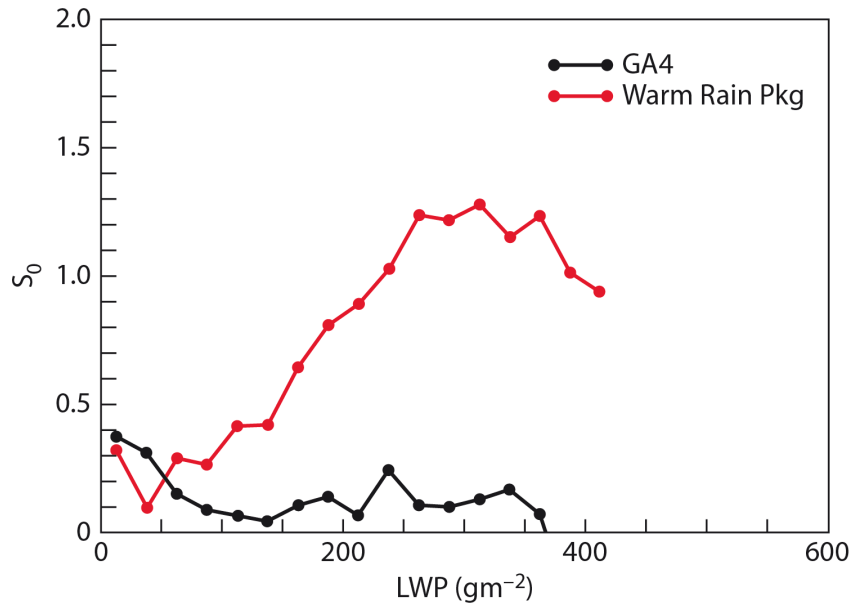


Figure 10. S_0 the GCM simulations with the UM using GA 4.0 (black) and the warm rain package (red)

Summary

We have presented an overview of recent work in which a kinematic model has been employed to aid the development, testing and comparison of the cloud microphysics schemes. It has been demonstrated that a kinematic framework is a very useful tool for understanding the underlying behaviour of a scheme without the complication of dynamic and radiative feedbacks. In this work we have focused on precipitation modelling by presenting

1. A comparison of the time evolution of surface precipitation from various microphysics schemes when cloud drop number concentration is 50 cm^{-3}
2. A comparison of certain parameters, e.g. maximum and accumulated precipitation, timing of precipitation for various N_d and LWP

Overall the comparison of schemes presented shows that the simplest single moment bulk schemes, 1M, tend to rain too early and have the least sensitivity to changes in N_d . By using the construct of precipitation susceptibility, S_0 , it is shown that the lack of sensitivity to N_d in the 1M scheme tested is probably unrealistic for the type of LWP simulated. There are caveats to such a conclusion, i.e. the value of S_0 for a given LWP and the exact behaviour over a range of LWP are uncertain; however, compared to other published work it seems that the low S_0 associated with the 1M scheme tested is not realistic. We have demonstrated how modifying the autoconversion scheme can improve S_0 relative to a bin scheme in a kinematic framework. It has also been demonstrated that employing more complex microphysics scheme, e.g. a 2M rain scheme or 2M cloud and rain, results in a more “realistic” S_0 . We have noted, however, that all the kinematic simulations with the bulk schemes tend to rain too early relative to the bin scheme. This is a feature that requires consideration if work is focused on high-resolution NWP or climate simulations where timing and location of precipitation is important.

References

- Abel, S. J. and Boutle, I. A. (2012), An improved representation of the raindrop size distribution for single-moment microphysics schemes. *Q.J.R. Meteorol. Soc.*, **138**: 2151–2162. doi: 10.1002/qj.1949
- Boutle I. A. and Abel S. J. 2012. Microphysical controls on the stratocumulus-topped boundary-layer structure during VOCALS-REx. *Atmos. Chem. Phys.* **12**: 2849–2863.
- Boutle, I. A., Abel, S. J., Hill, P. G. and Morcrette, C. J. (2013). Spatial variability of liquid cloud and rain: observations and microphysical effects. *Q. J. R. Meteorol. Soc.*, submitted.
- Khairoutdinov M. F., Kogan Y. L. 2000. A new cloud physics parameterization in a large-eddy simulation model of marine stratocumulus. *Mon. Weather Rev.* **128**: 229–243.
- Ryo Onishi and Keiko Takahashi, 2012, A Warm-Bin--Cold-Bulk Hybrid Cloud Microphysical Model, *J Atmos. Sci.*, **69**, pp.1474-1497
- Shipway and Hill, 2012, Diagnosis of systematic differences between multiple parametrizations of warm rain microphysics using a kinematic framework, *Q.J.R. Meteorol. Soc.*. doi: 10.1002/qj.1913.
- Thompson G, Field P. R., Rasmussen R. M., Hall W. D. 2008. Explicit forecasts of winter precipitation using an improved bulk microphysics scheme. Part II: Implementation of a new snow parameterization. *Mon. Weather Rev.* **132**: 519–542.
- Tripoli G. J., Cotton W. R. 1980. A numerical investigation of several factors contributing to the observed variable density of deep convection over south Florida. *J. Appl. Meteorol.* **19**: 1037–1063.
- Tzivion S, Feingold G, Levin Z. 1987. An efficient numerical solution to the stochastic collection equation. *J. Atmos. Sci.* **44**, 3139–3149.

